

Is Multiphase Gas Cloudy or Misty?

Max Gronke* and S. Peng Oh

Department of Physics, University of California, Santa Barbara, CA 93106, USA

Accepted 2020 February 11. Received 2020 February 5; in original form 2019 December 17

ABSTRACT

Cold $T \sim 10^4$ K gas morphology could span a spectrum ranging from large discrete clouds to a fine ‘mist’ in a hot medium. This has myriad implications, including dynamics and survival, radiative transfer, and resolution requirements for cosmological simulations. Here, we use 3D hydrodynamic simulations to study the pressure-driven fragmentation of cooling gas. This is a complex, multi-stage process, with an initial Rayleigh-Taylor unstable contraction phase which seeds perturbations, followed by a rapid, violent expansion leading to the dispersion of small cold gas ‘droplets’ in the vicinity of the gas cloud. Finally, due to turbulent motions, and cooling, these droplets may coagulate. Our results show that a gas cloud ‘shatters’ if it is sufficiently perturbed out of pressure balance ($\delta P/P \sim 1$), and has a large *final* overdensity $\chi_f \gtrsim 300$, with only a weak dependence on the cloud size. Otherwise, the droplets reassemble back into larger pieces. We discuss our results in the context of thermal instability, and clouds embedded in a shock heated environment.

Key words: galaxies: evolution – hydrodynamics – ISM: clouds – ISM: structure – galaxy: halo – galaxy: kinematics and dynamics

1 INTRODUCTION

Understanding the formation and dynamics of cold ($\sim 10^4$ K) gas is a crucial facet of galaxy formation. Cold gas not only fuels star formation, but (in contrast to the hot phase) it is detectable up to high redshift, and thus widely used as a probe of galactic outflows or the circumgalactic medium (e.g., [Veilleux et al. 2005](#); [Tumlinson et al. 2017](#)). However, despite its importance and ubiquity, cold gas around galaxies remains an enigma. It is present in galactic halos for a wide range of galaxy masses (e.g., [Steidel et al. 2010](#); [Wisotzki et al. 2016](#)), but its origin, perhaps from thermal instability or ejection from the galaxy, is poorly understood. Such cold gas should be vulnerable to disruption by hydrodynamic instabilities ([Klein et al. 1994](#); [Zhang et al. 2017](#)). Furthermore, it has been established observationally through multiple probes that circumgalactic cold gas can be structured on both small scales (< 100 pc, and potentially substantially less; e.g., [Rauch et al. 1999](#); [Churchill et al. 2003](#); [Schaye et al. 2007](#); [Hennawi et al. 2015](#)), and large scales (~ 100 kpc; e.g., [Werk et al. 2014](#)). The origin, survival, and morphology of cold gas are all outstanding puzzles.

Observationally, significant evidence for small-scale structure exists (e.g., reviewed in [McCourt et al. 2018](#), henceforth: [M18](#)), e.g., the order unity area covering fraction of dense gas in the CGM, despite the small volume filling fraction ($f_V \lesssim 0.1 - 1\%$). Theoretically, [M18](#) showed that when the cooling time falls far below the sound-crossing time in a cooling cloud, it becomes strongly underpressured relative

to surrounding hot gas, and ‘shatters’ to cloudlets of size $l_{\text{shatter}} \sim \min(c_s t_{\text{cool}}) \sim 0.1 \text{ pc } (n/\text{cm}^{-3})^{-1}$, akin to gravitational fragmentation to the Jeans length. Thus, ‘clouds’ of cold, atomic gas may have the structure of a mist, with tiny dispersed fragments embedded in ambient gas. [Sparre et al. \(2019\)](#) and [Liang & Remming \(2019\)](#) subsequently investigated 3D hydro and 2D MHD shattering in a wind-tunnel like setup respectively, while [Waters & Proga \(2019a\)](#) studied linear non-isobaric thermal instability.

On the other hand, in [Gronke & Oh \(2018, 2019\)](#) (also see [Li et al. 2019](#)), where we revisited cloud entrainment in a wind, we found that cold gas could survive hydrodynamic instabilities only if clouds *exceed* a critical lengthscale $r_{\text{min}} > c_s t_{\text{cool,mix}} \gg l_{\text{shatter}}$. This criterion arises from $t_{\text{cool,mix}} < t_{\text{cc}}$, where $t_{\text{cool,mix}}$ is the cooling time of the mixed warm gas and t_{cc} is the cloud-crushing time. In this regime, the cooling of mixed, ‘warm’ gas causes the cold cloud mass to grow. The cloud retains its monolithic identity; cold gas only survives as large ‘clouds’. The mass growth rate is similar in nearly static simulations with weak shear. The cloud pulsates due to loss of pressure balance seeded by radiative cooling, entraining hot gas which subsequently cools.

The ‘misty’ and ‘cloudy’ scenarios may appear mutually contradictory. However, terrestrially, we experience both; in the ISM and CGM, there is observational evidence for both. What is not known are the physical conditions under which cold gas should exist primarily in a ‘misty’ or ‘cloudy’ state, which we address here. This question has important consequences for the survival and dynamics of cold gas, the required resolution for a converged CGM & IGM in cosmological simulations ([van de Voort et al. 2019](#); [Hummels et al.](#)

* E-mail: maxbg@ucsb.edu, Hubble fellow

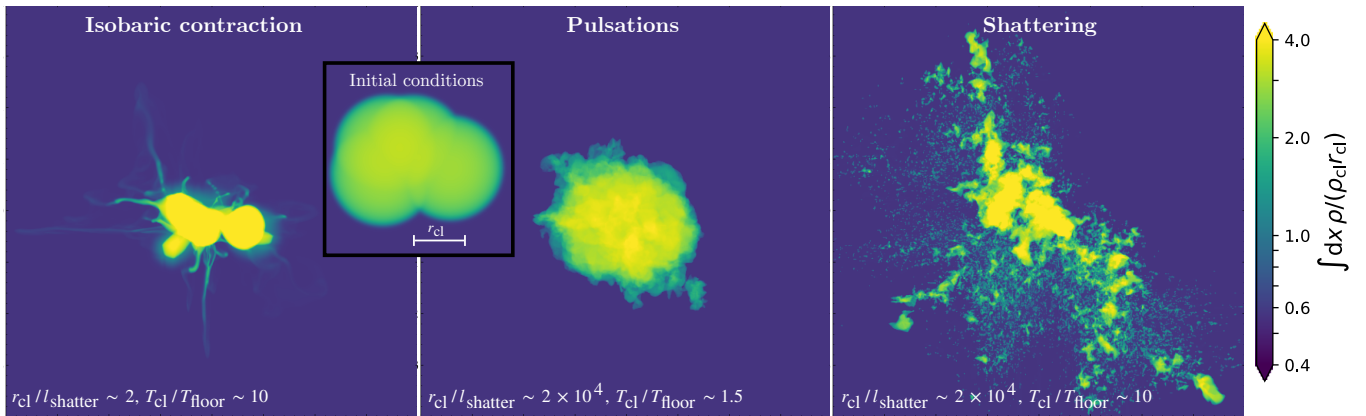


Figure 1. The outcome of different evolutionary paths of a cooling cloud, for a small cloud ($r_{\text{cl}} \sim \ell_{\text{shatter}}$; left panel), and large clouds ($r_{\text{cl}} \gg \ell_{\text{shatter}}$) which grow mildly (central) and strongly (right) out of pressure balance. Shown are the column densities of runs with $r_{\text{cl}}/l_{\text{cell}} \sim 64$; the parameters are stated in the bottom left corner of each panel, and the snapshots shown are at times (from left to right): $t \sim \{1, 9400, 860\}t_{\text{cool,cl}} \sim \{51, 7, 5\}t_{\text{sc,floor}}$. The inset shows the initial conditions to scale. While the small cloud in the left panel cooled isobarically, the larger clouds either pulsate (central panel) or shatter into tiny pieces (right panel), depending on the degree of pressure imbalance.

2019; Peebles et al. 2019; Mandelker et al. 2019), and radiative transfer and escape of ionizing and resonant line photons (e.g., Gronke et al. 2017).

2 NUMERICAL SETUP

‘Shattering’ appears to take place when a large ($r_{\text{cl}} \gg \ell_{\text{shatter}}$) cloud falls out of pressure balance with its surroundings. This occurs in at least two physical situations: (i) thermal instability, when the cloud pressure falls precipitously due to radiative cooling; (ii) a shock engulfing cold clouds, when the surrounding gas pressure rises sharply.

To simulate this, we placed four spherical clouds with radius r_{cl} and overdensity χ_i inside the simulation domain of size $8r_{\text{cl}}$ per dimension. We placed one cloud in the center, but displaced the three others with a maximum offset per dimension of r_{cl} (see inset in Fig. 1 for initial conditions). The deviation from spherical symmetry avoids the carbuncle instability (Moschetta et al. 2001), which seeds grid-aligned artifacts. We varied χ_i between 1.01 and 1000; the lower, (higher) value mimics a linear overdensity such as the origin of thermal instability, and cold gas embedded in a shock heated environment respectively. Furthermore, we perturb the density in every cell by a random factor r which is drawn from a Gaussian with $(\mu, \sigma) = (1, 0.01)$ (truncated at 3σ).

We set the initial cloud temperature to be $T_{\text{cl}} > T_{\text{floor}}$, where the cooling floor is $T_{\text{floor}} = 4 \times 10^4$ K and $T_{\text{cl}}/T_{\text{floor}}$ varies from 1.5 to 1000. The cloud is initialized to be in pressure balance with its surroundings, but rapidly falls out of pressure balance via radiative cooling. Since the cooling time is much shorter than the sound crossing time, the cloud cools isochorically to T_{floor} and $P_{\text{cl}}/P_{\text{hot}} \approx T_{\text{floor}}/T_{\text{cl}} < 1$. Thus, varying $T_{\text{cl}}/T_{\text{floor}}$ is equivalent to varying the degree of initial pressure imbalance; we tested this explicitly. The cloud can only regain pressure balance at a higher overdensity $\chi_f = \chi_i T_{\text{cl}}/T_{\text{floor}}$. We define $\ell_{\text{shatter}} \equiv c_{s,\text{floor}} t_{\text{cool}}(\rho_f, T_{\text{floor}})$.

To emulate heating of the background hot gas, we inhibited cooling for $T > 0.6T_{\text{hot}}$. We performed most of our simulations using $r_{\text{cl}}/l_{\text{cell}} = 16$ cell elements but we increased the resolution to $r_{\text{cl}}/l_{\text{cell}} = 64$ for some runs as indicated in the text. Note that we do *not* resolve ℓ_{shatter} in our simulations; shattering proceeds down to grid scale. While the

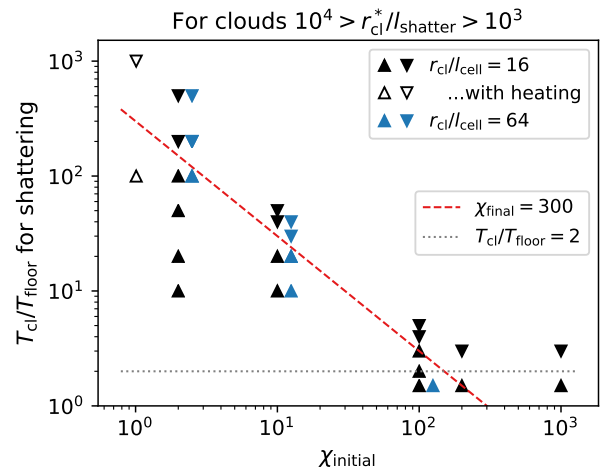


Figure 2. Conditions required for a large cloud to shatter. The triangles pointing downwards (upwards) show simulations that did (did not) shatter. The dashed line represents the final overdensity $\chi_f \approx (T_{\text{cl}}/T_{\text{floor}})\chi_i = 300$, which separates the two regimes. Open symbols represent runs with heating. $r_{\text{cl}}/\ell_{\text{shatter}} = 64$ are slightly shifted in x direction for clarity.

morphology of ‘shattered’ gas is not numerically converged, we have explicitly checked that our conclusions about the presence/absence of shattering, i.e., the fragmentation of the perturbed gas cloud (the focus of this paper) is numerically robust to resolution. We find that the resolution requirements to observe shattering are less stringent in 3D than in the 2D simulations of M18.

The simulations were run using Athena 4.0 (Stone et al. 2008) using the HLLC Riemann solver, second-order reconstruction with slope limiters in the primitive variables, and the van Leer unsplit integrator (Gardiner & Stone 2008), and the Townsend (2009) cooling algorithm (using a 7-piece powerlaw fit to the Sutherland & Dopita (1993) solar metallicity cooling function). The runtime of the simulations was max ($10t_{\text{sc,cl}}, t_{\text{cool,cl}}, 10t_{\text{cool,floor}}$), or until the cloud clearly shattered, with a significant number of droplets leaving the simulation domain. Animations visualizing our numerical results are available at <http://max.lyman-alpha.com/shattering>.

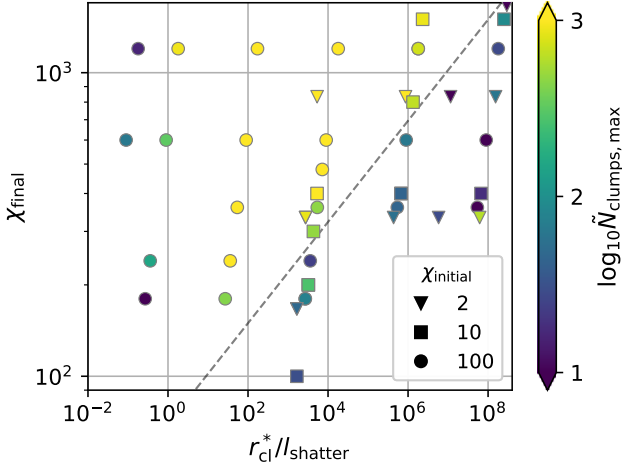


Figure 3. The resolution-adjusted maximum number of clumps identified during the runtime of a simulation, as a function of cloud size when sonic contact is lost (see text) and final overdensity χ_f . The number of clumps shows a sharp transition at χ_{crit} for ‘shattering’ given by the dashed line and $r_{\text{cl}} \sim \ell_{\text{shatter}}$ (see text for details). The marker shape indicates the initial overdensity χ_i . Points might be slightly offset for visualization.

3 RESULTS

Our simulations have 3 variables: cloud size, degree of pressure imbalance, and initial overdensity. Fig. 1 first shows graphically how cloud evolution changes with size and pressure contrast. The left panel shows a small cloud of size $r_{\text{cl}} \sim \ell_{\text{shatter}}$ with large pressure imbalance ($T_{\text{cl}}/T_{\text{floor}} \sim 10$), while the central and right panels show large clouds ($r_{\text{cl}} \gg \ell_{\text{shatter}}$) with small and large pressure imbalances respectively ($T_{\text{cl}}/T_{\text{floor}} \sim \{1.5, 10\}$). Clearly, both a large cloud *and* large pressure imbalance is required for shattering: only the simulation shown in the rightmost panel breaks up into small pieces. Interestingly, shattering does not happen during the initial compression by the surroundings, but only during an expansion phase. By contrast, the small cloud (left panel) never drastically loses sonic contact and contracts isobarically, while the large cloud with a smaller pressure imbalance (central panel) does not break up but instead oscillates (similar to what can be found in an entrained, growing cold gas cloud in a galactic wind at lower Mach numbers, where pressure variations are small; Gronke & Oh 2019).

What is the effect of the initial overdensity χ_i ? We first vary the parameters $(\chi_i, T_{\text{cl}}/T_{\text{floor}})$, holding cloud size $r_{\text{cl}} \gg \ell_{\text{shatter}}$ roughly constant. Fig. 2 shows the simulations which did and did not shatter, with triangles pointing downwards and upwards, respectively. Note that here, and below we define a simulation to ‘shatter’ if it broke apart to more than 100 pieces. Such fragmentation precludes reassembly back into a monolithic entity. A less overdense cloud needs to be more out of pressure balance (higher $T_{\text{cl}}/T_{\text{floor}}$) to shatter. The boundary between these regimes has a scaling $T_{\text{cl}}/T_{\text{floor}} \propto \chi_i^{-1}$, collapsing the criterion to a *single* parameter: the final overdensity must exceed a critical value $\chi_f \sim (T_{\text{cl}}/T_{\text{floor}})\chi_i > \chi_{\text{crit}} \sim 300$ to shatter. This requirement flattens out at large $\chi_i > \chi_{\text{crit}}$: at least $T_{\text{cl}}/T_{\text{floor}} \gtrsim 2$ (corresponding to $P_{\text{cl}} \lesssim 0.5P_{\text{hot}}$) is required. Note that the numerical value of χ_{crit} depends on parameters such as the

gas metallicity, and T_{floor} ; however, we expect the governing physics to be unchanged.

The case of lower initial overdensities ($\chi_i \lesssim 10$) requires special care. Since the initial cooling time is long at low densities, the cloud may initially retain sonic contact, that is $r_{\text{cl}} \lesssim c_{\text{s,cl}}t_{\text{cool}}(T_{\text{cl}}, \rho_{\text{cl}})$. However, since t_{cool} plummets as it cools and contracts, it will lose sonic contact at some point (since $r_{\text{cl}} \gg \ell_{\text{shatter}} \equiv c_{\text{s,floor}}t_{\text{cool}}(T_{\text{floor}}, \rho_{\text{floor}})$). The scale important for shattering is in fact the radius the cloud has when it loses sonic contact, which is $r_{\text{cl}}^* = \sqrt{\gamma P_0/\rho_*}t_{\text{cool}}(P_0/\rho_*, \rho)$ where P_0 is the ambient pressure and $\rho_* = \rho_{\text{cl}}(r_{\text{cl}}/r_{\text{cl}}^*)^3$ comes from mass conservation. We use r_{cl}^* to evaluate cloud size. If the cloud loses sonic contact before contraction (or never does), we set r_{cl}^* to r_{cl} .

Can shattering occur during thermal instability? This has not been shown to date; M18 began with non-linear initial conditions, $\chi_i \sim 10$. We simulated linear initial overdensities $\chi_i = 1.01$ and $T_{\text{cl}}/T_{\text{floor}} = \{10^2, 10^3\}$, where there is a long period of slow contraction. Here, we did not set the cooling function to zero above some temperature but instead introduced constant volumetric heating, set to equal the total cooling rate at each timestep. The cloud shatters, or does not, for $\chi_f \approx \{10^3, 10^2\}$ respectively (see unfilled triangles in Fig. 2), as expected since these bracket $\chi_{\text{crit}} \approx 300$.

Since $(T_{\text{cl}}/T_{\text{floor}}, \chi_i)$ collapse to the single variable χ_f , the entire parameter space can be viewed in the $(\chi_f, r_{\text{cl}}^*/\ell_{\text{shatter}})$ plane. In Fig. 3 we show how these two variables affect the maximum number of clumps which appear during the simulation. Larger clouds require higher resolution; the larger initial size $\chi_i \sim \{2, 10\}$ cases are run with $r_{\text{cl}}/l_{\text{cell}} = 64$ and only the $\chi_i \sim 100$ runs use the fiducial resolution of $r_{\text{cl}}/l_{\text{cell}} = 16$. To account for this, we use the rescaled variable $\tilde{N}_{\text{clumps,max}} = N_{\text{clumps}}r_{\text{cl}}/l_{\text{cell}}/64$. This shows a sharp transition at $\chi_{\text{crit}} \approx 300 \left(\frac{r_{\text{cl}}^*/\ell_{\text{shatter}}}{5000}\right)^{1/6}$ shown by the dashed line in Fig. 3. The exact scaling may change with resolution, but the conclusion that χ_{crit} scales only weakly with cloud size is robust.

What is the physical origin of shattering? We can gain insight by studying simulations which straddle the χ_{crit} boundary. Fig. 4 shows snapshots of two simulations, both with $\chi_i \sim 10$ and $r_{\text{cl}}^* \sim 5 \times 10^3 \ell_{\text{shatter}}$ but differing $T_{\text{cl}}/T_{\text{floor}}$, such that $\chi_f \sim 200$ and ~ 400 (upper and lower row, respectively). The clouds evolve as follows: (i) initially, they rapidly cool to the floor temperature. (ii) This leaves a large pressure imbalance leading to cloud contraction (first column). Note that the cloud does *not* shatter during the contraction phase, as one might expect. Instead, strong density perturbations and hot gas penetration arise due to Rayleigh Taylor instabilities similar to those which arise in supernovae, except this is an implosion rather than an explosion. The pressure in the cloud overshoots that of the surroundings, leading to (iii) a rapid expansion phase (second column). As it expands, the cloud (iv) fragments into smaller pieces (‘shatters’; third column). This shattering is likely driven by Richtmyer-Meshkov instabilities as the expansion front sweeps over the strong density inhomogeneities created during the contraction phase, creating strong vorticity and breaking up the cloud. We tested this by allowing a similarly overpressurized but uniform cloud to rapidly expand; in this case shattering does *not* occur.

Crucially, the cloud evolution now diverges. As seen in the fourth and fifth columns of Fig. 4, the cloudlets can either (v;

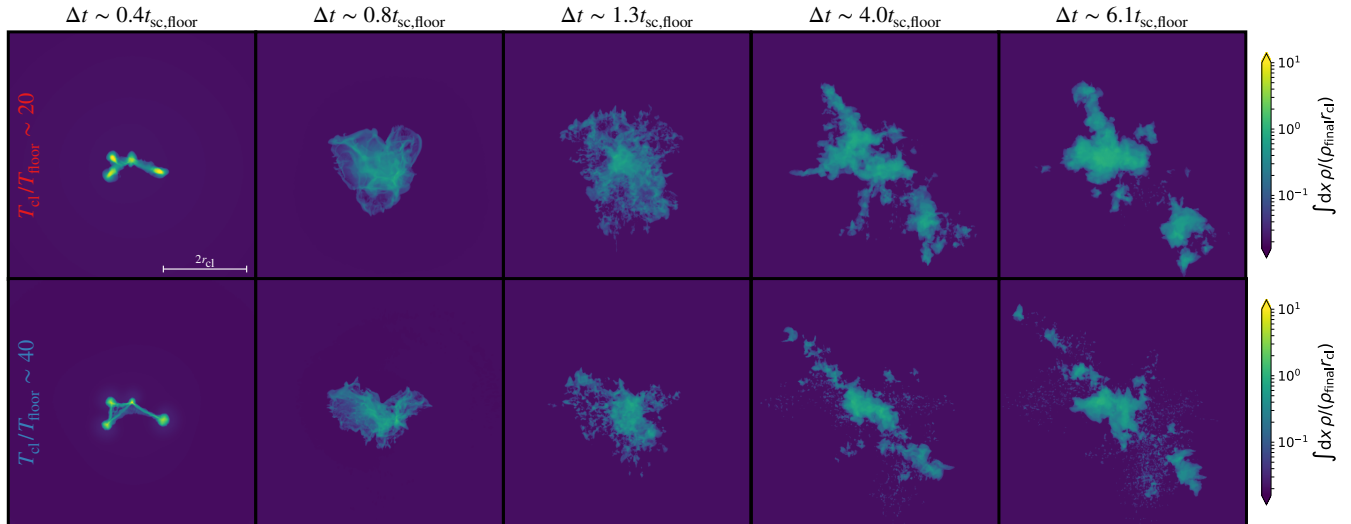


Figure 4. The evolution of shattering. The upper (lower) row shows snapshots from simulations with $\chi_i \sim 10$ and $T_{cl}/T_{floor} \sim \{20, 40\}$, and thus $\chi_f \sim \{200, 400\}$ respectively. The time Δt is measured relative to the first contraction. Each row shows the process of initial contraction, expansion (with clear fragmentation), shattering (leading to the formation of many “droplets”), and finally coagulation – where the droplets merge back again onto the larger cold gas structures. The simulation with the larger χ_{final} (shown in the lower row) shows less merging as can also be seen in Fig. 5 (where the line color matches the labels in the first panel of this figure).

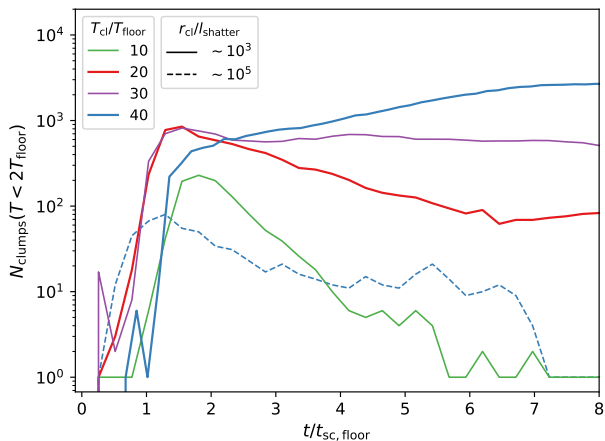


Figure 5. The number of clumps (with $T < 2T_{floor}$) as a function of time for simulations with $\chi_i \sim 10$ but different χ_f and cloud sizes (denoted by the color and linestyle, respectively). The thicker lines (in red & blue) are the simulations shown in Fig. 4. While all clouds break up into small pieces initially, the efficiency of subsequent coagulation determines the final outcome.

a) disperse in the surrounding of the original cloud (bottom panels), or (*v*; *b*) fall back and coagulate into larger clouds (top panels). The remaining (or re-forming) larger clouds (*vi*) continue to pulsate. This process is accompanied by a significant mass growth as entrained hot gas cools, as in Gronke & Oh (2018, 2019). For instance, the $T_{cl}/T_{floor} \sim 20$ (~ 40) cloud depicted in Fig. 4 has roughly tripled (doubled) its mass at $t \sim 6t_{sc,floor}$.

Thus, while ‘shattering’ always begins in a large cloud out of pressure balance, whether it prevails depends on a competition between breakup and coagulation. This can be quantitatively seen in Fig. 5 where we show the number of cloudlets as a function of time. The solid lines depict $r_{cl}/\ell_{shatter} \sim 10^3$ (for which $\chi_{crit} \sim 300$), and $\chi_f = \{1, 2, 3, 4\} \times 100$. These all show

fragmentation into $\gtrsim 100$ pieces at $t \sim 2t_{sc,floor}$, the point of maximum expansion. However, for $\chi_f < \chi_{crit}$, the droplets coagulate, reversing the shattering process. The dashed line shows that coagulation is more efficient for a larger cloud (i.e. χ_{crit} increases).

4 DISCUSSION & CONCLUSIONS

In this work we revisit the ‘shattering’ mechanism first identified by M18 in 2D simulations; we now do so in 3D. Our simulations are governed by 3 dimensionless parameters: the initial cloud overdensity χ_i , the initial cloud size $r_{cl}/\ell_{shatter}$, and the pressure contrast $P_{cl}/P_{hot} \approx T_{floor}/T_{cl}$. As anticipated, we find that a cloud must be large ($r_{cl}/\ell_{shatter} \gg 1$) and out of pressure balance ($P_{cl}/P_{hot} \lesssim 0.5$) to shatter. However, we also find an unexpected requirement that the final overdensity $\chi_f \gtrsim \chi_{crit} \approx 300$, with a weak scaling on cloud size. Otherwise, the fragments quickly merge. For $T_{floor} \sim 10^4$ K, this suggests that shattering is inefficient in gas with $T_{hot} < 3 \times 10^6$ K. We also show that shattering occurs during linear thermal instability $\delta\rho/\rho \ll 1$. It has hitherto only been shown for large, non-linear overdensities.

We find ‘shattering’ is really a spectrum spanned by the dispersal of cloudlets and their merger. On the ends of this spectrum lie clouds which ‘explode’, violently launching the droplets in all directions, and clouds where the restoring coagulation force is so strong that they never break up but instead pulsate. In between, the fate of cold gas depends on the competition between breakup and coagulation, which is governed by the final overdensity χ_f . Coagulation was already seen in the original 2D simulations of M18 (see their fig. 3, third panel from top; fig. 6, and associated discussion), but its true importance is only now apparent.

What drives coagulation? There are at least two causes: (i) radiative cooling, which drives pressure gradients in mixed interstitial gas, the source of mass growth discussed in Gronke & Oh (2018, 2019). Cooling-induced coalescence has also been

highlighted in Elphick et al. (1991); Waters & Proga (2019b), though merger velocities seen in those low overdensity ($\chi \sim \text{few}$) calculations are much smaller than seen there, requiring $\gtrsim 10^3 - 10^4$ cooling times for coalescence, and could not compete with breakup. (ii) Turbulence. It is well known that clumping instabilities driven by particle inertia or wave-particle resonance operate in dust-gas interactions (e.g., Lambrechts et al. 2016; Squire & Hopkins 2018), and may also operate in cloudlet-gas interactions.

Without a quantitative understanding of coagulation, we cannot derive a criterion for shattering. Nonetheless, it seems physically reasonable that the competition between ‘launching’ and ‘drag’ depends on overdensity χ_f (which sets the particle stopping length). For coagulation driven by cooling, we can make the following heuristic argument. Suppose that the dispersion of cloudlets is set by the RM instability. The hot gas punches through pressure gradients with a characteristic velocity $c_{s,\text{hot}}$, and cold clouds disperse with a characteristic velocity $\sim \alpha c_{s,\text{hot}}$, where α encodes imperfect entrainment. Over a cloud oscillation time, the cloudlets disperse over a volume $l_{\text{launch}}^3 \sim (\alpha c_{s,\text{hot}} t_{\text{sc, floor}})^3$. On the other hand, the volume of interstitial hot gas which is consumed by the cloudlets over this time is $V_{\text{hot}} \sim \dot{m} t_{\text{sc, floor}} / \rho_{\text{hot}} \sim r_{\text{cl}}^3 (r_{\text{cl}} / \ell_{\text{shatter}})^{1/4}$, where we have used the mass entrainment rate $\dot{m} \sim r_{\text{cl}}^2 \rho_{\text{hot}} v_{\text{mix}}$ where $v_{\text{mix}} \sim c_{s,\text{floor}} (t_{\text{cool, floor}} / t_{\text{sc, floor}})^{-1/4}$ (Ji et al. 2019; Gronke & Oh 2019). For the cloudlets to disperse faster than interstitial hot gas can be consumed, we require $l_{\text{launch}}^3 \gtrsim V_{\text{hot}}$. Using $c_{s,\text{hot}} / c_{s,\text{floor}} \sim \chi_f^{1/2}$ yields $\chi_f \gtrsim \alpha^{-2} (r_{\text{cl}} / \ell_{\text{shatter}})^{1/6}$, which fits our results for $\alpha \sim 0.12$ (cf. dashed line in Fig. 3).

Besides thermal instability, our setup can also mimic cold clouds (with large $\chi_i \gtrsim 100$) engulfed by a shock, where the background pressure rises rapidly. Using the shock jump conditions, one can relate $\chi_{\text{crit}} \sim \max(300, 3\chi_{\text{initial}})$ to a requirement for the Mach number of the wind in order for the cloud to shatter: $\mathcal{M}^2 \gtrsim [(\gamma + 1)\chi_{\text{crit}} / \chi_i + (\gamma - 1)] / (2\gamma)$, which corresponds to $\mathcal{M} \sim 1.6$ for $\chi_i \gtrsim 100$. This is roughly consistent with our wind-tunnel setup in Gronke & Oh (2019) where our fiducial $\mathcal{M} = 1.5$ setup was numerically converged, while the higher Mach-number runs (with $\mathcal{M} = 3$ and $\mathcal{M} = 6$) were not. We attributed this to the larger compression of the cloud, but breakup via shattering can also drive resolution requirements. In the $\mathcal{M} \sim 1.5$ runs, a solid ‘tail’ behind the cloud forms quickly, while the tail in $\mathcal{M} = 6$ simulation is much more diffuse and transient.

Regardless, the competition between breakup and coagulation will differ when there are background gas motions. It is not at all clear that clouds subject to a wind can both shatter *and* survive; the pieces need to coagulate into larger fragments ($> c_s t_{\text{cool, mix}}$) to survive (e.g., as in fig. 6 of M18). It may well be that while clouds can entrain and grow in transonic winds, they do not survive higher Mach number winds, where shattering into small fragments dominates. The impact of background turbulence is also unclear: it could drive fragmentation, or clumping and coagulation (as for dust). These issues require high resolution simulations with careful attention to convergence. Our physical understanding of the shattering/coagulation mechanisms, and their interaction with extrinsic turbulence, magnetic fields, and cosmic rays, remain tenuous. It will be the subject of future work.

ACKNOWLEDGMENTS

We thank Yan-fei Jiang, Drummond Fielding, Brent Tan and particularly Dongwook Lee for discussions on numerical issues, and the referee for helpful comments. This research made use of yt (Turk et al. 2011). We acknowledge support from NASA grants NNX17AK58G & HST-HF2-51409, HST grant HST-AR-15039.003-A, and XSEDE grant TG-AST180036. MG thanks JHU for hospitality.

REFERENCES

- Churchill C. W., Mellon R. R., Charlton J. C., Vogt S. S., 2003, *ApJ*, 593, 203
- Elphick C., Regev O., Spiegel E. A., 1991, *MNRAS*, 250, 617
- Gardiner T. A., Stone J. M., 2008, *J. Comput. Phys.*, 227, 4123
- Gronke M., Oh S. P., 2018, *MNRAS*, 480, L111
- Gronke M., Oh S. P., 2019, *MNRAS*, in press,
- Gronke M., Dijkstra M., McCourt M., Peng Oh S., 2017, *A&A*, 607, A71
- Hennawi J. F., Prochaska J. X., Cantalupo S., Arrigoni-Battaia F., 2015, *Science*, 348, 779
- Hummels C. B., et al., 2019, *ApJ*, 882, 156
- Ji S., Oh S. P., Masterson P., 2019, *MNRAS*, 487, 737
- Klein R. I., McKee C. F., Colella P., 1994, *ApJ*, 420, 213
- Lambrechts M., Johansen A., Capelo H. L., Blum J., Bodenschatz E., 2016, *A&A*, 591, A133
- Li Z., Hopkins P. F., Squire J., Hummels C., 2019, *MNRAS*, p. 3180
- Liang C. J., Remming I., 2019, *MNRAS*, p. 3032
- Mandelker N., van den Bosch F. C., Springel V., van de Voort F., 2019, *ApJ*, 881, L20
- McCourt M., Oh S. P., O’Leary R., Madigan A.-M., 2018, *MNRAS*, 473, 5407
- Moschetta J.-M., Gressier J., Robinet J.-C., Casalis G., 2001, *Godunov Methods: Theory and Applications*. Springer US, Boston, MA, pp 639–645
- Peeples M. S., et al., 2019, *ApJ*, 873, 129
- Rauch M., Sargent W. L. W., Barlow T. A., 1999, *ApJ*, 515, 500
- Schaye J., Carswell R. F., Kim T.-S., 2007, *MNRAS*, 379, 1169
- Sparre M., Pfrommer C., Vogelsberger M., 2019, *MNRAS*, 482, 5401
- Squire J., Hopkins P. F., 2018, *ApJ*, 856, L15
- Steidel C. C., Erb D. K., Shapley A. E., Pettini M., Reddy N. A., Bogosavljević M., Rudie G. C., Rakic O., 2010, *ApJ*, 717, 289
- Stone J. M., Gardiner T. A., Teuben P., Hawley J. F., Simon J. B., 2008, *ApJS*, 178, 137
- Sutherland R. S., Dopita M. A., 1993, *ApJS*, 88, 253
- Townsend R. H. D., 2009, *ApJS*, 181, 391
- Tumlinson J., Peeples M. S., Werk J. K., 2017, *ARA&A*, 55, 389
- Turk M. J., Smith B. D., Oishi J. S., Skory S., Skillman S. W., Abel T., Norman M. L., 2011, *ApJS*, 192, 9
- Veilleux S., Cecil G., Bland-Hawthorn J., 2005, *ARA&A*, 43, 769
- Waters T., Proga D., 2019a, *ApJ*, 875, 158
- Waters T., Proga D., 2019b, *ApJ*, 876, L3
- Werk J. K., et al., 2014, *ApJ*, 792, 8
- Wisotzki L., et al., 2016, *A&A*, 587, A98
- Zhang D., Thompson T. A., Quataert E., Murray N., 2017, *MNRAS*, 468, 4801
- van de Voort F., Springel V., Mandelker N., van den Bosch F. C., Pakmor R., 2019, *MNRAS*, 482, L85

This paper has been typeset from a $\text{\TeX}/\text{\LaTeX}$ file prepared by the author.